광산지질 제14권 4호 (1981) pp. 183-191

Origin of Massive Amphibolitic Rocks in Imgye Area, Korea

Chil-Sup So, Youn-Ki Kim, Se-Jung Chi and Maeng-Eon Park

Abstract : Major and trace elements analyses are presented for 13 amphibolites by wet chemical and emission spectroscopic methods. These chemical data were compared with limestone and quartzite closely associated with the amphibolites. The chemical similarity of the amphibolites studied to the basic igneous rock and low oxidation ratios (<30) are indicative of the igneous intrusive, especially middle stage differentiates. Petrographic and stratigraphic study of the rocks suggest the more igneous features rather than those of sedimentary progenitors.

Introduction

The studied area situated in the eastern part of the Ogcheon geosynclinal zone is underlain mainly by Precambrian quartzite of Taebaegsan series and Jangsan quartzite and Great Limestone series of Chosun group and, to the east, by Jurrasic granite. The amphibolites studied occur as massive body along the border zone of the above rock series (Fig. 1).

Some study of the mafic matamorphic rocks was carried out by members of the Geological Survey of Korea mainly from the viewpoint of petrography and stratigraphy, but they had not yet studied enough on the origin and chemistry of the amphibolites. Recently So and Kim (1974) suggest the igneous origin of the Imgye amphibolites by their geochemical consideration of the rock on the Ogcheon geosynclinal zone.

The studied area contains some silver deposits closely associated with the amphibolites. The writers have attempted to find nature and origin of the amphibolites of the area and to contribute to an understanding of their close association to the silver deposits, using the geochemical methods outlined by Evans and Leake (1960) and Leake (1964). All the geochemical data of the rocks studied were compared with the amphibolites in the Ogcheon geosynclinal zone.

Sampling and treatment

Sampling was designed to obtain materials representative of all parts of the rocks. Specimens each weighing 1-2 kg were collected. Sampling localities are shown in Figure 1.

All specimens were examined petrographically, and modal analyses were done with a Swift Automatic Point Counter on unstained thin sections, and the results are given in Table 1. Counting interval of 1/6×2mm was used, and generally at least 1,000 points were counted in each section. Measurements of the refractive index of hornblende were done by using standard liquids on cleavage fragments. The index of refraction of the liquid was checked on an Abbe Refractometer immediately after each match was obtained. In most thin sections the plagioclase was so poorly twinned and so highly sericitized that no satisfactory measurements could be made.

Sampling were prepared for chemical and spectroscopic analyses by slicing the rocks across the foliation and breaking these into 3-1 inch chips. The chips were broken to sand-size grains in a jaw crusher prior to being powdered in a shatter box with a tungsten carbide grind-

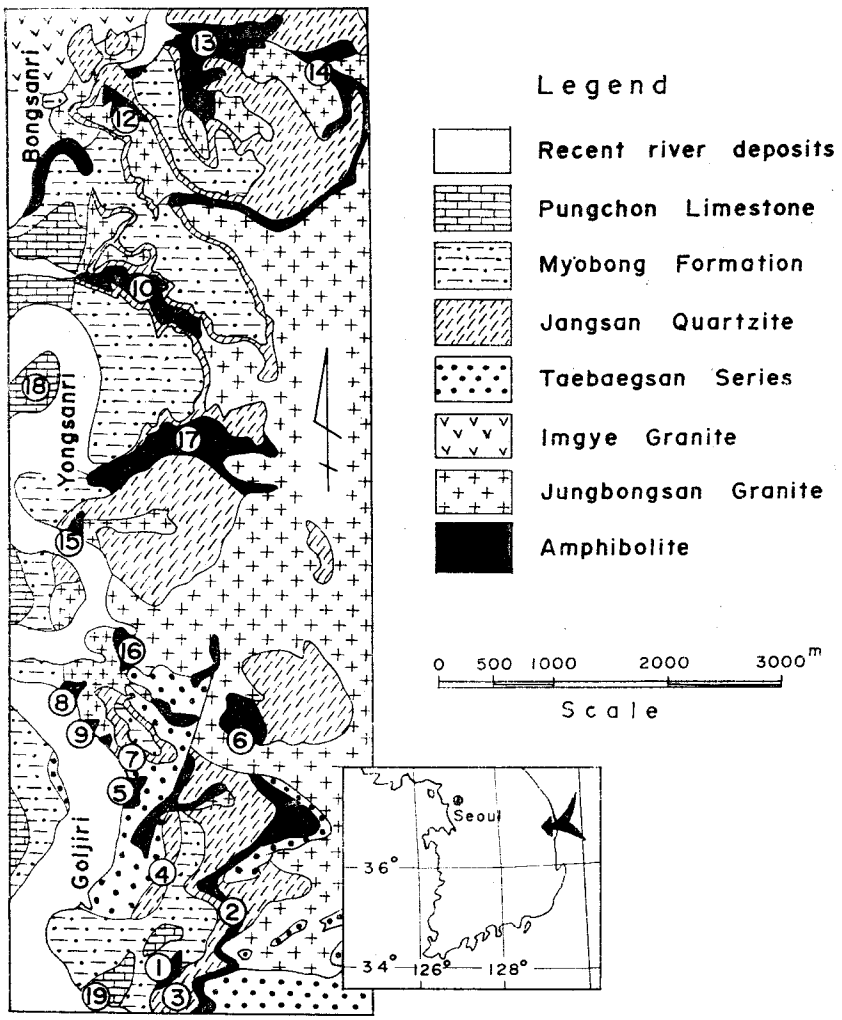

Fig. 1 Simplified geological map showing the sampling localities.

ing container (100ml). The powders were ground until all passed through a 150-mesh (105μ) sieve.

Analytical methods

Chemical analysis: The oxides of silicon, iron (Ⅲ), calcium, magnesium and aluminum were determined by gravimetric method after alkali fusion. Ferrous oxide was extracted into saturated aqueous solution of boric acid and was titrated with permanganate solution. Determination of phosphorous was conducted by colorimetry using vanadomolybdate reagent. Potassium and sodium were analyzed by Perkin-Elmer 303 atomic absorption spectrophotometer. Copper was analyzed by colorimetry. Determination of titanium was done by X-ray fluorescence spectrometry using a Phillips electronic instrument.

Spectrochemical analysis : Each prepared sample was mixed with a buffer (NaCl+Carbon powder SP-3) free from spectroscopic impurities. A crater in the lower positive electrode

(National SPKL-3703) of highest purity graphite was filled with the sample mixture. Arc spectra of the amphibolites were recorded on Eastman Kodak SA-1 plates using a 3.4 meter grating spectrograph, Jarrell-Ash Ebert mounting, with dispersion in the first order of 5.1 Å per mm. Comparison with master plate determined the qualitative presence of minor elements. Comparison with spectra of ratio powders which contain known quantities of interesting elements fixed the order of magnitude of manganese, chromium, cobalt, nickel, vanadium and strontium.

Petrography and field relationships of the amphiboltes

The studied area is underlain by the Taebaegsan series, Jangsan quartzite, Myobong formation, Pungchon limestone, biotite granite intrusives and amphibolites with minor occurrence of basic dykes. The Taebaegsan series is distributed chiefly the south of area and overlain unconformably by Jangsan quartzite. It consists of alternation of gray quartzite, fine-grained quartz-biotite gneiss, quartz-plagioclase-biotite gneiss, brown biotite hornfels and banded biotite-plagioclase-quartz gneiss. Jangsan quartzite consists of mainly gray to buff and milky white quartzite and contains pebbles in few localites. It is intruded by amphibolite at the base in some places. Myobong formation comprised dark gray to greenish black slate, phyllite, schist and gray limestone. The formation overlies conformably Jangsan quartzite. Pungchon limestone overlies conformably Myobong formation and consists mainly milky white massive and crystalline limestone. These rocks are interlayed occasionally by black shales.

Jungbongsan granite around Jungbongsan penetrated into Taebaegsan series and Jangsan quartzite. The granite also intrudes into amphibolite sills or dykes that penetrated into Taebaegsan series and Myobong formation, and is in turn penetrated by Imgye granite. These granites are mostly biotite granite and their lithologics are similar each other.

Massive amphibolites crop out predominantly within the quartzite and limestone. Main amphibolite unit is several hundreds of meters in thickness and several kilometers in length.

Table 1. Modal analyses

	Minerals (Vol. %)											Counts Pointed	Traverse Sp. mm	Ref. Index of Hornblende	
	Hornblende	Plagioclase	Quartz	Biotite	Pyroxene	Chlorite	Calcite	Sphene	Epidote	Apatite	Opaques			$N\alpha$	N_β
1	45	4	34	6	—	1	—	2	1	2	5	1017	1/6×2	1.660	1.676
2	68	15	6	6	—	1	—	1	1	—	3	1127	1/6×2	1.654	1.682
5	71	12	11	1	—	1	—	1	1	—	3	1360	1/6×2	1.656	1.680
6	65	14	13	2	—	1	—	1	3	—	1	1120	1/6×2	1.660	1.686
8	61	20	8	5	1	—	—	2	2	1	1	1094	1/6×2	1.664	1.686
9	54	24	16	3	—	—	—	1	1	—	2	1109	1/6×2	1.664	1.684
10	62	15	11	4	—	1	1	2	4	—	1	1087	1/6×2	1.662	1.694
12	68	12	10	2	—	1	1	4	1	—	1	1210	1/6×2	1.666	1.686
13	41	9	29	13	—	1	1	3	2	1	1	1101	1/6×2	1.666	1.688
14	31	22	25	7	—	—	1	5	3	1	5	1007	1/6×2	1.668	1.688
15	52	21	14	2	2	—	—	2	5	—	2	1017	1/6×2	1.668	1.686
16	53	25	9	5	—	1	—	3	2	—	2	1039	1/6×2	1.664	1.690
17	54	28	12	—	1	1	—	1	1	—	3	1237	1/6×2	1.666	1.690

Table 2. Chemical and emission spectroscopic analyses, Niggli values and oxidation ratios

	1	2	3	4	5	6	7	8	9	10	12	13	14	15	16	17	18	19
SiO_2(%)	50.40	53.10	73.80	60.90	52.80	52.00	67.10	52.10	49.30	52.30	55.30	52.70	56.20	48.40	56.00	54.00	3.88	4.50
Al_2O_3	18.70	16.40	14.50	21.90	17.60	18.00	16.30	18.30	18.10	17.90	16.00	16.10	17.40	18.10	17.00	17.40	0.24	0.13
Fe_2O_3	8.69	1.43	0.39	1.40	1.10	3.83	0.87	5.27	4.83	1.56	1.70	4.33	5.30	3.82	0.73	1.65	0.60	0.34
FeO	5.58	9.84	2.50	4.85	9.55	7.49	5.88	5.88	5.88	9.11	8.81	6.61	4.55	5.29	8.81	8.81	N.D	N.D
MnO	0.33	0.08	0.17	0.28	0.19	0.21	0.18	0.19	0.19	0.18	0.03	0.17	0.001	0.04	0.17	0.19	0.01	0.03
MgO	6.58	6.63	2.31	3.69	5.88	5.68	3.32	6.34	7.56	6.44	6.16	6.22	4.90	6.13	5.55	5.36	0.80	0.54
CaO	5.13	8.22	1.63	1.17	8.63	8.40	0.58	7.12	7.70	7.87	6.16	9.54	7.06	9.49	8.02	8.47	51.60	51.60
Na_2O	2.92	1.36	1.84	2.84	2.24	2.08	2.28	2.16	3.16	2.32	2.12	2.16	1.78	2.08	1.98	2.36	N.D	N.D
K_2O	1.00	1.40	1.20	0.80	1.20	1.44	1.32	1.00	2.50	0.88	2.00	0.84	1.28	5.60	1.12	1.30	N.D	N.D
TiO_2	0.01	0.02	tr	tr	0.02	0.02	tr	0.01	0.01	0.01	0.01	0.01	0.01	0.02	0.01	0.01	tr	tr
P_2O_5	0.01	0.01	0.01	0.01	0.01	0.01	0.01	0.01	0.01	0.01	0.01	0.01	0.01	0.01	0.01	0.01	tr	tr
Ig.loss	0.68	1.18	1.44	2.24	0.83	0.65	1.84	1.27	1.00	1.20	1.49	1.09	1.00	0.62	0.70	1.04	42.6	42.4
Total	100.03	99.67	99.69	100.08	100.05	99.81	99.68	99.65	100.24	99.78	99.79	99.78	99.491	99.60	100.10	100.60	99.73	99.53
Ni(ppm)	62.0	24.0	136.0	104.0	80.0	58.0	34.0	68.0	132.0	112.0	108.0	86.0	118.0	74.0	66.0	120.0	210.0	38.0
Cr	82.0	184.0	64.0	90.0	88.0	84.0	92.0	74.0	90.0	78.0	146.0	70.0	58.0	86.0	75.0	66.0	-	4.8
Co	100.0	296.0	88.0	68.0	94.0	76.0	70.0	60.0	86.0	140.0	46.0	94.0	78.0	38.0	86.0	80.0	-	-
Cu	120.0	76.0	170.0	34.0	90.0	60.0	260.0	180.0	27.0	190.0	75.0	216.0	250.0	150.0	44.0	30.0	23.0	20.0
Sr	100.0	28.0	112.0	94.0	120.0	94.0	100.0	88.0	76.0	100.0	-	94.0	104.0	-	94.0	100.0	410.0	330.0
Ba	725.5	275.4	985.6	2015.5	254.8	398.7	1215.4	242.4	287.6	250.5	432.5	338.5	500.4	487.6	405.4	287.9	12.5	13.5
La	8.5	6.5	7.0	5.0	5.0	4.0	6.5	15.0	4.0	4.0	4.0	4.0	4.0	4.0	4.0	4.0	6.5	5.0
Sc	22.5	17.8	19.2	10.5	19.7	23.8	9.8	18.6	22.5	23.0	24.8	24.5	20.4	22.5	20.5	21.8	7.8	7.5
V	65.5	35.5	6.2	7.0	65.0	65.0	6.0	19.5	18.7	43.5	53.5	25.7	38.5	50.5	52.3	63.5	1.2	2.5
Rb	60.0	20.0	50.0	180.0	12.0	15.0	100.0	70.0	65.0	30.0	70.0	50.0	60.0	85.0	100.0	50.0	20.0	18.0
Zr	58.5	48.7	60.5	50.2	49.5	51.4	95.2	42.4	48.7	55.8	50.5	48.5	46.4	47.5	48.7	49.5	1.5	1.8
K/Rb	70.0	294.0	100.8	18.7	420.0	403.2	55.4	60.0	161.5	123.2	120.0	70.6	89.6	276.7	47.0	109.2	-	-
si	122.10	133.07	393.98	215.51	131.02	128.93	280.24	131.41	115.68	144.51	148.57	129.97	158.74	112.81	149.01	137.74	6.80	7.97
al	26.65	24.06	45.53	45.59	25.69	26.25	40.04	27.15	24.98	26.10	25.29	23.36	28.91	24.80	26.61	26.11	0.25	0.13
fm	51.65	48.33	31.54	38.44	44.08	44.16	44.63	41.73	46.99	46.04	48.04	44.96	42.70	38.46	43.53	42.80	2.91	1.93
c	13.32	22.07	9.33	4.44	22.95	22.32	2.60	19.24	19.36	20.90	17.73	25.20	21.37	23.70	22.86	23.15	96.84	97.94
alk	8.38	5.54	13.60	11.53	7.28	7.27	12.73	6.88	8.67	6.96	8.94	6.48	7.02	13.02	7.00	7.94	-	-
k	0.18	0.40	0.30	0.16	0.26	0.31	0.28	0.23	0.17	0.20	0.38	0.20	0.33	0.64	0.27	0.27	-	-
mg	0.46	0.52	0.59	0.51	0.50	0.48	0.47	0.51	0.57	0.52	0.52	0.51	0.49	0.56	0.51	0.48	0.72	0.74
ti	0.02	0.04	-	-	0.03	0.03	-	0.01	0.01	0.02	0.01	0.01	0.02	0.03	0.01	0.01	-	-
p	0.01	0.01	0.02	0.01	0.02	0.01	0.01	0.01	0.01	0.01	0.01	0.01	0.01	0.01	0.01	0.01	-	-
Oxid. Ratio	58.36	11.57	9.44	20.62	9.40	31.52	11.76	44.65	42.58	13.35	14.80	37.09	51.19	39.20	6.94	14.42		
Field Occur.	●	●	▣	▣	●	●	▣	●	●	●	●	●	●	●	●	●	△	△

● Amphibolite
▣ Quartzite
△ Limestone

$$\text{Oxidation Ratio} = \frac{2Fe_2O_3 \times 100}{2Fe_2O_3 + FeO} \quad \text{(Oxides in mols)}$$

The amphibolites of the area are medium-to coarse-grained varieties consisting of hornblende, quartz, plagioclase together with minor components such as biotite, sphene, epidote, pyroxene, chlorite, calcite, apatite. Subhedral hornblende is z-light greenish and greenish and has average grain sizes ranging from 0.1 $\times$0.2mm to 0.3$\times$0.5mm. Refractive indices of hornblende are 1.654−1.668 (Nα) and 1.676−1.694 (Nα). Fine hornblendes are randomly distributed around the larger one. Anhedral quartz grains are aggregated and some are often included in the hornblende. Plagioclase is commonly altered to sericite and chlorite. Small euhedral biotite, reddish brown in color, is distributed randomly and some are often found as an retrograde products from hornblende. Chlorite, calcite and epidote are the alteration products of the hornblende. Anhedral sphene and opaques are intimately associated with hornblende.

Geochemical results

Major elements: All the chemical data on the amphibolites were recalculated into Niggli values, and these values were correlated with the field occurrence of the amphibolites and are shown in various diagrams.

In recent papers, Evans and Leake (1960) and Leake (1964) have emphasized the difference between sedimentary and igneous trends in plots such as Niggli *c* against *mg* and 100*mg*–*c*–(*al*–*alk*), and the usefulness of such plots in determining whether a suite of amphibolites is of igneous or of sedimentary origin. Figures 2 and 3 are two such plots for the Imgye amphibolites. In the diagrams the field occupid by the striped ortho-amphibolites of Connemara (Leake, 1964) is shown, as well as the area occupied by pelitic rocks (Shaw, 1956), and the points representing three quartzites and two limestones from Imgye. From these two figures, and especially from the *c* versus *mg* plot, one can see that the supposed ortho-amphibolites of Imgye area plot together respective of the field occurrences and follow fairly well the igneous trend of the Karroo dolerites.

It can also be seen that nearly all of the studied amphibolites occupy a small area within

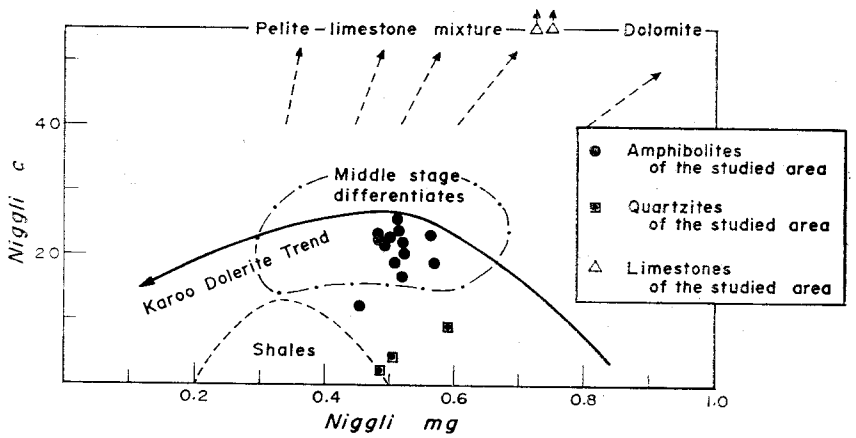

Fig 2. Niggli *mg* versus *c* plot.

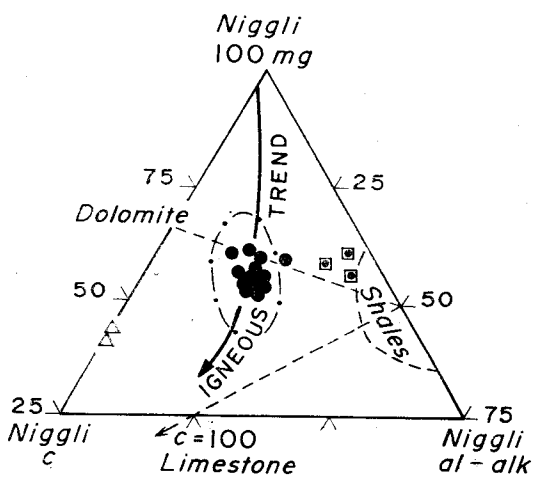

Fig. 3 Niggli values plotted on a 100*mg*–*c*–(*al*–*alk*)diagram.

the Connemara striped amphibolites. The closer grouping given by the rocks in the *c* versus *mg* and in the 100*mg*–*c*–(*al*–*alk*) plots, as well as their general agreement with the igneous trend of the Karroo dolerites, suggest the middle stage differentiates.

In Figures 4 and 5, plots of *al*–*alk* versus *c*, and the *k* and *alk* against *mg* Niggli values are given. Here again the amphibolites from Imgye plot together as a well defined group within the area of the ortho-amphibolites. In three of the plots, however, there is a considerable overlap between the field of pelites and that of the ortho-amphibolites, and

both *c* and *al-alk* are strongly dependent upon the mode. The plots presented in Figures 4 and 5 are not so useful, in distinguishing ortho-from para-amphibolites.

Recently, So (1974) presented a new model for the origin of the amphibolites in Gyeonggi metamorphic complex. In the present study, the Imgye amphibolites have a small range of *si* values (112.81−158.74)and show the Niggli *mg* and *c* values (0.46−0.57 and 13.32−25.

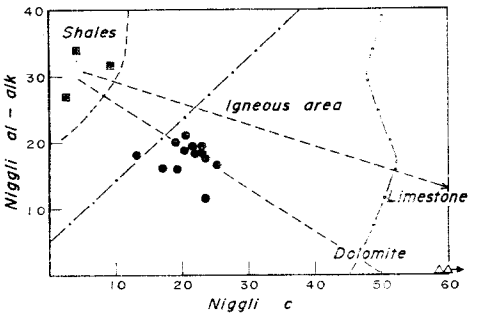

Fig. 4 Niggli *al-alk* versus *c* plot.

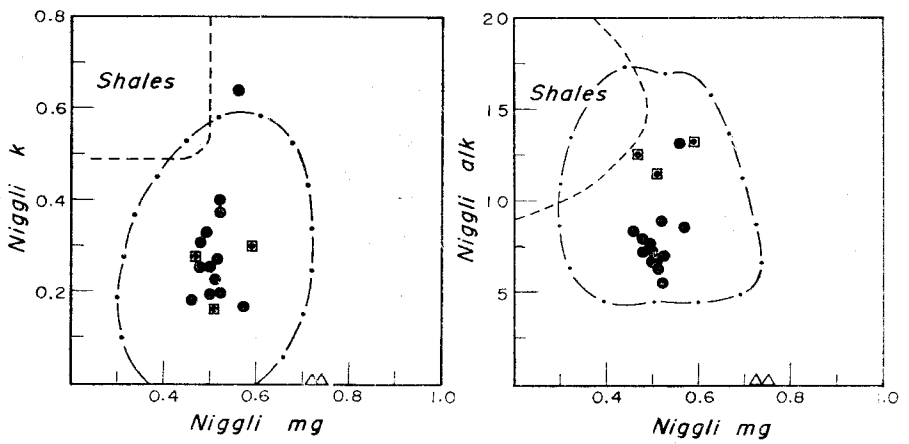

Fig. 5 Niggli *k* and *alk* versus *mg* plots.

20) which are much lower than that of the limestone (0.72−0.74 and 96.84−97.94). Figure 6 displays such distinct variation trend.

Figure 7 is the plots of Niggli *mg* and *fm* against Niggli *al*+*alk*+*si*. The lack of variation of the *mg* values of the rocks plotted to *al*+*alk*+*si* suggest that the amphibolites in the Imgye area did not accompany the removal or influx of major elements during the formation of the rocks, and the major elements are useful enough in determining the origin of the rocks.

Minor elements: Trace element abundances are the most independent of the mode and of alteration of the rocks, Evans and Leake (1960), and Leake (1964) indicated that amphibolites rich in Cr, Ni, and Ti, and having low *k* values are almost certainly igneous in origin, but amphibolites having low Cr, Ni, and Ti values and high *k* values can be either igneous or sedimentary in origin. Cr and Ni are the most useful minor elements in distinguishing igneous from sedimentary. In Ni and Cr versus Cu plots(Fig. 8), the rocks from the Imgye area plot in the area of igneous region or in the transitional part of the ortho-and para-amphibolite region (Ni, 58-132 ppm except 1 sample and Cr, 58-184 ppm).

In the differentiation of basic igneous rocks, a decrease in *mg* is accompanied by a marked decrease in Cr and Ni, whereas mixtures of pelite and dolomite or limestone become more rich in Cr and Ni with decrease in *mg*, i.e. with decrease in the proportion of dolomite, because both limestone and dolomite are chara-

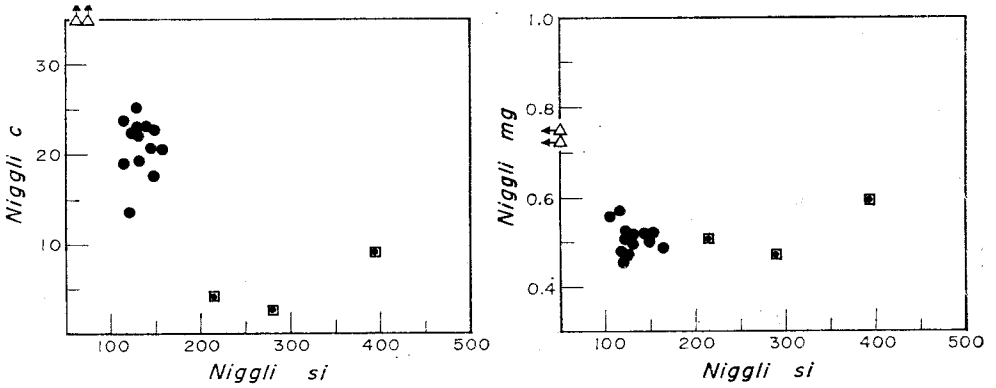

Fig. 6 Niggli *mg* and *c* versus *si* plots.

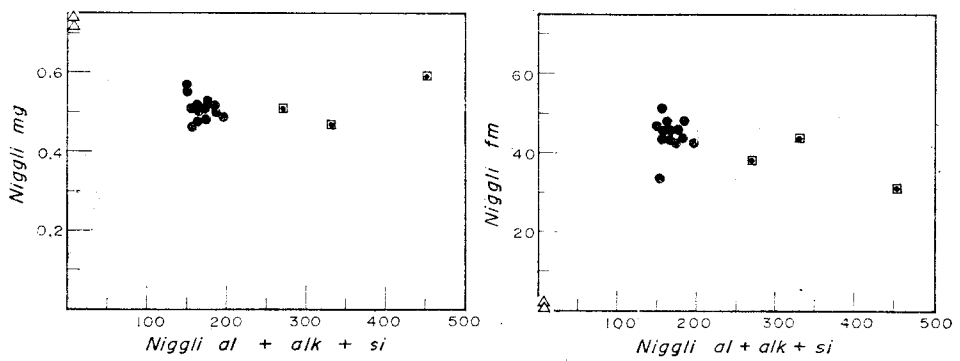

Fig. 7 Niggli *mg* and *fm* versus *al*+*alk*+*si* plots.

cteristically poor in these trace elements compared with pelites. Thus there should be two opposite trends for ortho-and para-amphibolites. The chromium and nickel plotted against *mg* of the rocks studied show a sympathetic positive correlation similar to those for basic igneous rocks and opposite to those for pelite-carbonate mixture (Fig. 9).

Further evidence for the derivation of the Imgye amphibolites is shown in K/Rb versus K (%) plot (Fig. 10), which show trend similar to those for the amphibolites studied by Kamp (1971). Rubidum abundance in the amphibolites is generally less than 100ppm as compared to the range of the Green Beds amphibolites as plotted by Kamp (1970).

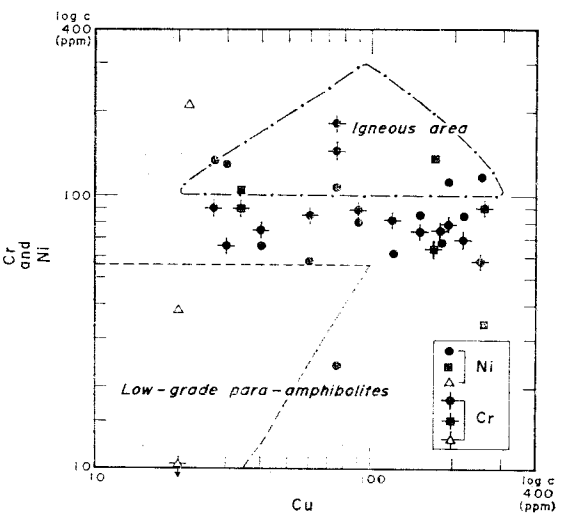

Fig. 8 Log-log plot of Cu versus Cr and Ni.

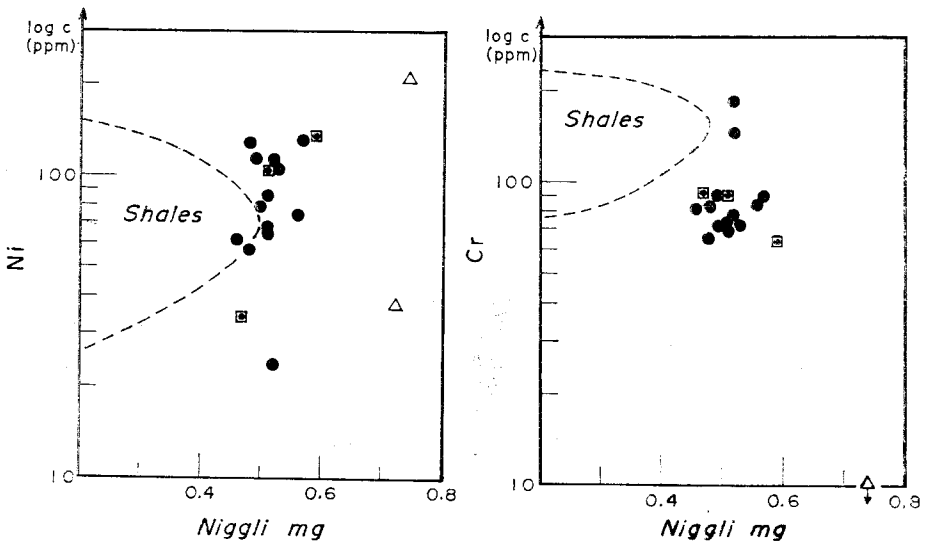

Fig. 9 Semi-log plots of Niggli *mg* versus Cr and Ni.

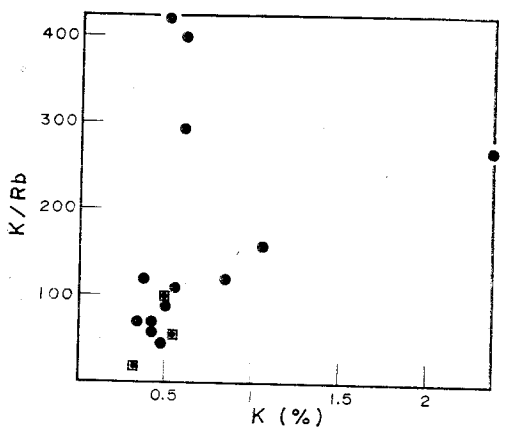

Fig. 10 K/Rb plotted against K (%).

Origin of the amphibolites

The above presentation is based on considerations of the bulk composition of the amphibolites and on the presupposition that during metamorphism individual rocks acted essentially as closed systems (Fig. 7). All the geochemical results from the above diagrams indicate agreement with petrogaphic observation and field criteria that the studied amphibolites are formed from basic igneous rocks, particularly middle stage differentiates.

The lower oxidation ratio (<30), that is, mols, $2Fe_2O_3\times100/2Fe_2O_3+FeO$, of the studied rocks are more typical of intrusives than of extrusive or sedimentary rocks.

References

Evans, B. W., and Leake, B. E. (1960) The Composition and Origin of the Striped Amphibolites of Connemara, Ireland: Jour. Petrology, v. 1, p. 337–368.

Kamp, van de, P. C. (1970) The Green Beds of the Scottish Dalracliam series: Geochemistry, Origin, and Metamorphism of Mafic Sediments: Geol. Soc. America Bull., v. 80, p. 1127.

Kamp, van de, P. C. (1971) A Precambrian Conglomerate with an Amphibolite Matrix Near Kaladar, Ontario: Jour. Geol. Soc. v. 127, p. 563–577.

Leake, B. E. (1964) Chemical Distinction of Ortho- and Para-amphibolites: Jour. Petrology, v. 5, p. 237–254.

So, C. S. (1974) Geochemistry and Origin of Amphibolites in Gyeonggi Metamorphic Belt, Korea: Jour. Geol. Soc. Korea, v. 10, p. 189–205.

So, C. S., and Kim, S. M. (1975) Geochemistry,

Origin, and Metamorphism of Mafic Metamorphic Rocks in the Ogcheon Geosynclinal Zone, Korea: Geol. Soc. Korea, v. 11, p. 115-137.

So, C. S., and, Kim S. M. (1975) The Chemistry and Origin of Amphibolitic Rocks in the Sobaegsan Metamorphic Belt and the Ogbang and Sangdong Tungsten Mine Area, Korea: Jour. Korean Inst. Mining Geol., v. 8, p. 147-164.

So, C. S., and Kim, S. M., and Son, D. S. (1975) Origin of the Magnetite-Bearing Amphibolites from the Yangyang Iron Mine, Korea: New Geochemical data and Interpretation: Jour. Korean Inst. Mining Geol., v. 8, p. 175-182.

So, C. S., and Son, D. S. (1976) The Chemistry and Origin of the Amphibolites of the Pocheon Iron Mine, Korea and their Close Association with Magnetite Ore: Jour. Korean Inst. Mineral and Mining Engineers, v. 13, p. 37-46.

臨溪地域에 分布하는 角閃石質岩의 成因

蘇 七燮, 金 然基, 池 世定, 朴 孟彦

要約：沃川地向斜內의 동북부에 위치한 臨溪지역의 角閃石質岩은 그 産出狀態가 塊狀이며 곳에따라 주변암석과 非相合的으로 보이나 아직까지 이들 암석에 대한 成因究明은 전무한 상태이고, 부근에는 많은 銀鑛床이 부존되어 있어 이들 암석의 정확한 成因究明은 매우 중요할것으로 사료된다. 蘇 七燮(1975)에 의한 본지역 몇 角閃石質岩 시료의 地化學的인 고찰은 火成起源으로 사료되었으나 그 대상시료가 소수여서 만족할만한 결과를 얻지 못한바, 본 연구에서는 많은 시료의 主成分및 稀有元素들의 變化경향(variation trend), 절대적 함량을 야외산출상태및 鑛物學的인 연구와 병행하여 이미 밝혀진 국내외의 여러 角閃石質岩들과 비교 검토함으로써 그 成因을 밝혔다. Niggli 값을 사용한 각종 도면에서 본 岩石들은 鹽基性 火成岩類의 中期分化物의 地化學的인 특성을 암시하며, 稀有成分으로서 Ni (58~132ppm) 및 Cr (58~184 ppm)의 함량은 火成起源의 trend를 보여준다. 또한 모든 시료에서 나타난 oxidation ratio (<30)도 貫入岩의 특징을 나타내 주고있다. 이들의 결과는 旣히 연구된 外國의 正-角閃石質岩(Evans and Leake, 1960. Leake, 1964)및 국내 正-角閃石質岩의 연구(蘇 七燮, 1974, 1975, 1976) 결과와도 일치한다.